Modulating Emission Properties in a Host-guest Colloidal Quantum Well Superlattice

*Junhong Yu[1+], Manoj Sharma[1,2,5+], Yimeng Wang[1], Savas Delikanli[1,2], Hamed Dehghanpour Baruj[2], Ashma Sharma[1], Hilmi Volkan Demir[*1,2,3], Cuong Dang[*1,4]*

[1]LUMINOUS! Centre of Excellence for Semiconductor Lighting and Displays, School of Electrical and Electronic Engineering, The Photonics Institute (TPI), Nanyang Technological University, 50 Nanyang Avenue, 639798, Singapore

[2]Department of Electrical and Electronics Engineering and Department of Physics, UNAM-Institute of Materials Science and Nanotechnology, Bilkent University, Bilkent, Ankara, 06800, Turkey

[3]School of Physical and Mathematical Sciences, Division of Physics and Applied Physics, Nanyang Technological University, 639798, Singapore

[4]CINTRA UMI CNRS/NTU/THALES 3288, Research Techno Plaza, 50 Nanyang Drive, Border X Block, Level 6, 637553, Singapore

[5]ARC Centre of Excellence in Exciton Science, Department of Materials Science and Engineering, Monash University, Clayton Campus, Melbourne, Victoria 3800, Australia

[+]These authors contribute equally

* Email: volkan@stanfordalumni.org; hcdang@ntu.edu.sg

Abstract: Self-assembly of colloidal nanocrystals into ordered superlattices is a powerful approach to enable novel collective properties which are not available in individual colloids. However, to date, it remains a major challenge to develop a practical route to modulate such collective properties for potential photonic applications. Herein, we show that the collective emission properties in colloidal quantum well (CQW) superlattices, including emission colour and anisotropy, can be effectively modulated in a binary host-guest architecture. The experimental and theoretical results reveal that excitons of the host (i.e., the undoped CQWs) generated by photoexcitation can be controllably harvested by the guest (i.e., the Cu-doped CQWs) for light emission, owing to an exciton hopping assisted exciton trapping process. Such a nano-building block with tuneable collective optical properties may enlighten novel colloidal material-based photonic applications, including optical anti-counterfeiting, next-generation liquid crystal displays, and multi-functional biological markers.

Superlattices constructed by colloidal nanocrystals, which mimic the organization of atoms into a crystal and exhibit unique ensemble properties, have attracted tremendous research interests for the design of novel functional materials[1-4]. Besides the common advantages of the colloidal nanocrystal family to be ingredients to construct superlattices[5,6], such as wide tunability in geometry/physical properties and easy-to-handle colloidal states, colloidal quantum wells (CQW) have demonstrated exceptional photophysical properties benefitting from the atomically flat nanostructure and its magic-sized vertical thickness[7-14]. These characteristics, including spectrally pure light emission[7,8], preferential interactions between the platelet planes[9-11] and a highly anisotropic electronic structure[12-14], have highlighted CQWs as a promising type of building blocks to generate superlattices targeting for photonic applications.

So far, considerable progress in the investigations of CQW superlattices has been made by different groups[9,10, 15-20]. Long anisotropic CQW superlattices beyond 10 μm have been observed and the collective properties of the ordered superlattices have been characterized. For example, Murray *et al.* demonstrated that the self-assembly of CQWs can be directed into ordered superlattices at the liquid-air interface[15,16]. Tisdale *et al.*[13] and Riedinger *et al.*[18] revealed that the orientation of CQWs in the superlattice can be controlled by engineering the solvent.

Dubertret *et al.* showed that the self-assembly of CQWs into stacked columnar structures displays polarized emission[9] and a phonon-replica line at low temperature[10]. However, the majority of these efforts on CQW superlattices have focused on structure constructions and understandings of emerging properties. To functionalize the CQW superlattices for photonic applications, it is often desirable to self-assemble the CQWs into a superlattice with programmable collective properties[21]. Unfortunately, this controllability has remained elusive and a daunting challenge to date.

In this work, we propose a binary host-guest superlattice constructed by 4 monolayers (MLs) CdSe undoped (the host) and Cu-doped CQWs (the guest) to demonstrate the modulation of collective emission properties. Experimental results reveal that the presence of even a few guest ingredients can strongly modify the preference of exciton recombination channel via band-edge emission (BE) or copper emission (CE) due to an ultralong exciton hopping range (> 100 nm)[17,20] and an ultrafast exciton hopping rate (~ 4 ps)[11,17, 22]. By enlarging the vertical dimension of the binary superlattice, more photoexcited excitons are harvested by Cu dopants and as a result, the greenish and anisotropy photoluminescence (the intrinsic emission properties of BE)[12,13] is gradually changed into the reddish and isotropy photoluminescence (the intrinsic emission properties of CE)[22,23]. In addition, we have modelled the excitonic dynamics (including exciton transfer, exciton trapping and exciton recombination) in the binary superlattice, which can well-reproduce the controllability observed in the experiments. This work, which expands the current understanding of manipulating collective properties in colloidal superlattices, could lead to novel photonic applications such as multimode optical anti-counterfeiting, next-generation liquid crystal displays, and multi-functional biological markers.

RESULTS AND DISCUSSION

Undoped CdSe CQWs with a vertical thickness of 1.2 nm corresponding to 4 MLs of lattice unit are synthesized according to previously reported procedures[7,24]. After thorough purification, the undoped CQWs covered with oleic acid ligands are dispersed in hexane. As shown in the left panel of **Fig. 1a**, the quantum confinement in the vertical direction of undoped CQWs enables two sharp excitonic transitions, which correspond to the electron/light-hole (maxima at 480 nm) and electron/heavy-hole (maxima at 512 nm) absorption features (top panel of **Fig. 1b**). Due to the ultrafast relaxation of light-holes to heavy-holes (<1 ps)[25,26], only greenish BE emission peaked at 514 nm associated with electron/heavy-hole exciton recombination can be observed in the emission spectrum (the top panel of **Fig. 1b**). Imaging by transmission electron microscopy (TEM) shows that the undoped CQWs have a monodisperse size distribution and a flat square-like shape with an average size of 22±5 nm (**Fig. S1a**), supporting the formation of long-range ordered superlattices.

Copper ions doped into CdSe CQWs can be realized by using both nucleation doping and partial cation exchange[22,27-30]. However, the nucleation doping method generally results in rectangular-shaped CQWs which are difficult for long-range stacking. For this work, we prefer doped and undoped CQWs with similar dimensions to construct the binary superlattice, therefore, we follow our earlier report on partial cation exchange recipes, where we add a controllable amount of copper acetate precursor into a solution of square-shaped undoped 4 ML core CQWs[28]. It is worth mentioning that under the studied doping range, copper dopants modify neither the geometry of the CQWs (see **Fig. S1b**) nor the essential excitonic absorbance of the CQWs. One can see in the bottom panel of **Fig. 1b**, both electron/heavy-hole and electron/light-hole transitions remain unchanged. Here, the role of copper dopants is to introduce emissive mid-gap states into the CQW host, as shown in the right panel of **Fig. 1a**. After photoexcitation, the heavy-holes can be trapped by the copper sites ($Cu^{1+} + h \rightarrow Cu^{2+}$, h denotes the heavy-hole), and then CE (a broad reddish emission band in the bottom panel of **Fig. 1b**) is activated by the recombination between the captured holes in copper dopants and the electrons in the conduction band of the host CQWs: $Cu^{2+} + e \rightarrow Cu^{1+} + h\nu$ ($h\nu$ is the photon energy of CE and e denotes an electron)[23,31,32].

We mix the undoped and Cu-doped CQWs dispersed in hexane (the concentration of both is 10 mg/mL) into a total of ~3 mL volume with an undoped-to-doped molar ratio of 10. Previously, various groups (e.g., Dubertret[9,10], Demir[17,20] and Abécassis[33]) have demonstrated that adding polar solvents such as ethanol into the CQW dispersions, which are dissolved in nonpolar solvents (such as hexane here), can lower the interaction potentials between the platelet planes of CQWs because the nonpolar capping ligands will force the CQWs to minimize the surface energy to draw away these added polar solvents[13,20]. Therefore, a relatively strong van der Waals attraction between the platelet planes induces the CQWs to stack on top of each other and results in a column-like superlattice.

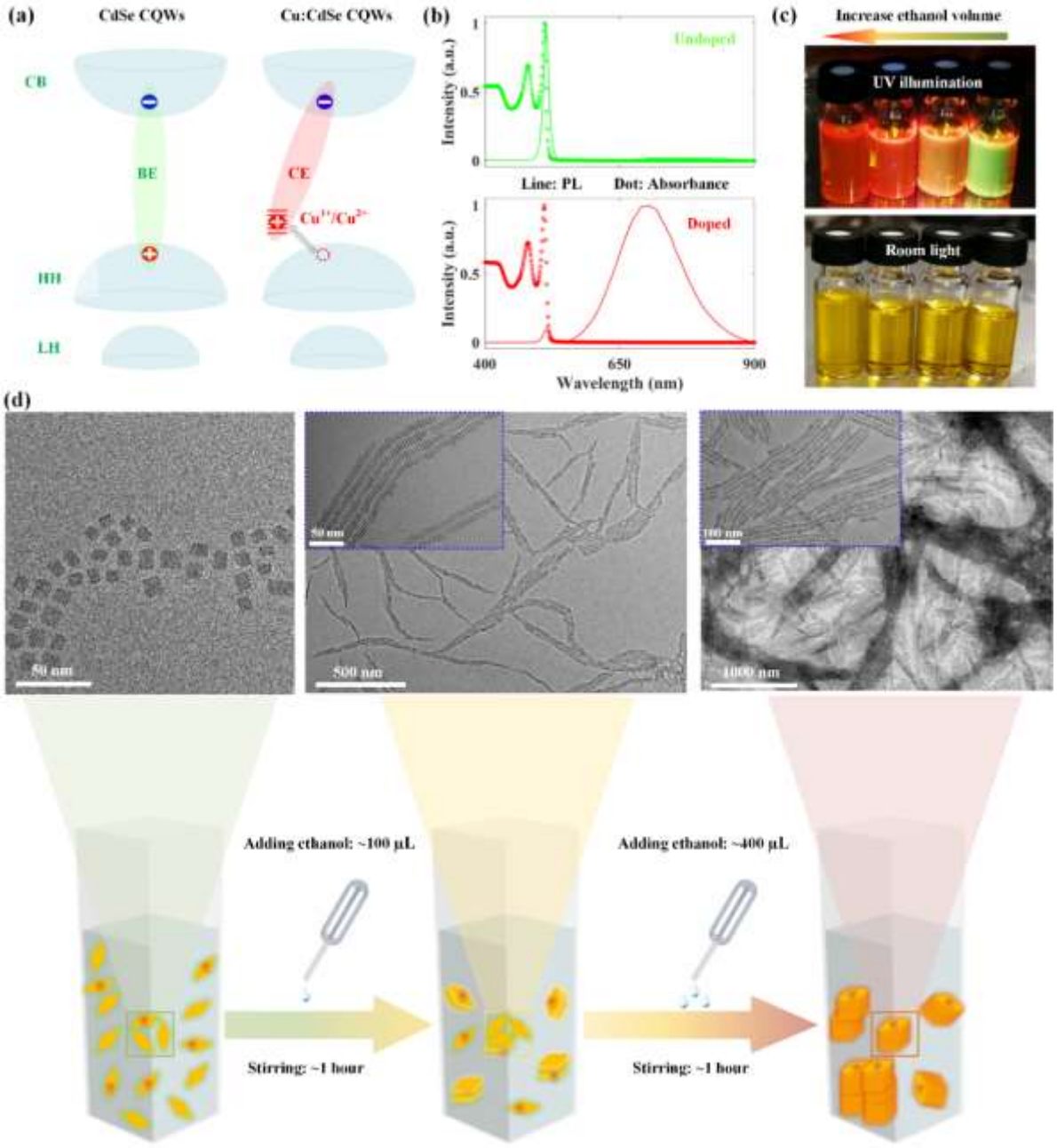

Figure 1. The formation of binary CQW superlattices. (a) Schematic illustrations of the excitonic processes in undoped CQWs (the left panel) and Cu-doped CQWs (the right panel). CB: conduction band, HH: heavy-hole, LH: light-hole. **(b)** Absorption and photoluminescence spectra of undoped CQWs (the top panel) and Cu-doped CQWs (the bottom panel). **(c)** Colour pictures of the binary CQW mixture dispersed in hexane with different amounts of added ethanol under 365 nm UV lamp (the top panel) and under room light (the bottom panel). From right to left: the volume of ethanol added into the binary mixture is 0, 100, 200, and 400 µL, respectively. **(d)** Schematic of adding ethanol to obtain CQW superlattices with different stacking degrees and corresponding TEM images of the binary CQWs. As the volume of ethanol is increased gradually, longer and heavier stacking of CQWs into columnar superlattices is observed.

Here we adopt the same method to initiate the stacking. To control the degree of stacking, different amounts of ethanol are added to the same pristine mixture. We observe that when a larger amount of ethanol is added into the binary mixture, after stirring for a while, the solution becomes more turbid, suggesting the formation of macroscale particles[9]. More interestingly, by tuning the volume of added ethanol, the emission colours of the binary mixture can be modified. Specifically, under UV illumination as shown in **Fig. 1c**, the pristine mixture is greenish since the majority of emitters are undoped CQWs; however, the colour of the mixture changes from green to red with more ethanol added, indicating that CE is dominating the emission process. Note that all these four solutions look yellowish under room light. At this point, a legitimate question would be whether the added ethanol changes the intrinsic properties of CQWs. To rule out this possibility, we have investigated again the

absorption and emission spectra of the mixtures after adding ethanol. The results in **Fig. S2** reveal that: two excitonic transition features are still located at 480 and 512 nm. Also, the peak position as well as the full-width at half-maximum (FWHM) of both BE and CE display negligible changes. The only changing factor is the intensity ratio between CE and BE. Thus, we can attribute the observed modification to the formation of superlattices.

To better understand the formation of CQW superlattices and characterize the degree of stacking, TEM micrographs of the mixtures with different amounts of ethanol addition are exhibited in **Fig. 1d**. For the pristine mixture (i.e., no ethanol added, see the left TEM panel), all CQWs are in the face-down configuration and no discernible stacking can be observed. When 100 μL of ethanol is added into the mixture (see the middle TEM panel), sparsely microwire-like superlattices, in which CQWs are edged-up in a highly aligned columnar order and the principal axis of the superlattice (i.e., the axis along the superlattice) is perpendicular to the platelet plane of CQWs, are detected. As the volume of ethanol increased to 400μL (see the right TEM panel), we notice that almost all CQWs are assembled into the stacking manner to form the superlattices. Even in the direction parallel to the platelet plane of CQWs, more than 10 columns of stacked CQWs with a width larger than 100 nm are standing side by side to form a giant superlattice. It is worth mentioning that small-angle X-ray scattering (SAXS) measurements can further confirm the formation of the ordered superlattice and extract the average center-to-center distance between two adjacent CQWs[9,33-35].

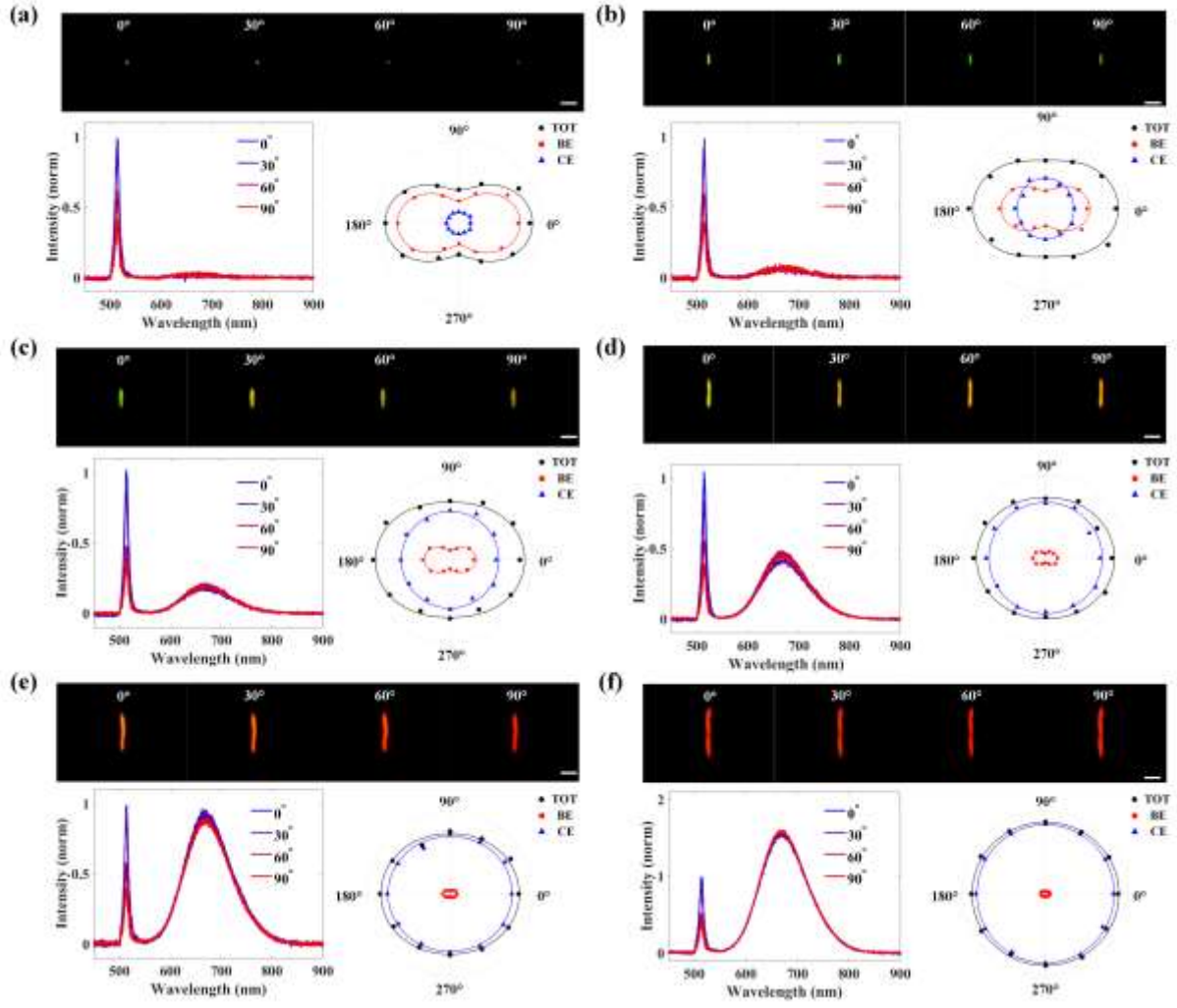

Figure 2. Emission colour and anisotropy in the binary CQW superlattices with different stacking lengths. Photoluminescence microscopy images (above), angle-dependent emission spectra (the lower-left panel) and angular polarization profiles of emission (the lower right panel) of the binary superlattice with a length of **(a)** ~1.4 μm, **(b)** ~3.8 μm, **(c)** ~6.7 μm, **(d)** ~9.8 μm, **(e)** ~13.4 μm and **(f)** ~17.2 μm. All are excited by a continuous-wave laser (405 nm) with a linear polarization perpendicular to the principal axis of superlattices. The angle between detection polarization and excitation polarization is indicated. In the emission images, the scale bar is 5 μm. The plotted data in angular profiles are fitted with a sinusoidal function. TOT: normalized integrated intensities of the full (total) emission spectra.

At the aim of providing convincing evidence that the controllability is resulting from the formation of superlattices, it is essential to extract the emission properties of a single superlattice from the ensemble photoluminescence (PL) profile of the dispersion which contains multiple superlattices with different stacking levels[36]. To ensure only an individual superlattice is characterized, after adding 200 μL ethanol, a diluted binary mixture dispersion is sparsely deposited onto a glass substrate via drop-casting. Then, each specific superlattice is excited by a linearly-polarized continuous-wave laser (405 nm) with polarization perpendicular to the principal axis of the superlattice, i.e. parallel to platelet planes. The emission is collected by an angle-resolved polarized μ-PL set-up (see experimental details in **Methods**) to probe the colour and anisotropy[9,37,38]. Six superlattices with different stacking lengths have been characterized and the optical images recorded by a CMOS camera allow us to determine the length value. The results of superlattices with lengths of 1.4, 3.8, 6.7, 9.8, 13.4 and 17.2 μm are presented in **Fig. 2**. The emission images and spectra of the single superlattice have exhibited consistency with our previous observation in superlattice dispersion (see **Fig. 1c** and **Fig. S2**): the stacking length can modify the intensity ratio between BE/CE and a longer superlattice will display the emission colour closer to red. Great attention is paid to the angle-resolved polarized emission properties (see the angular polarization profiles in the lower right panel of **Fig. 2**). For all these six superlattices with different stacking lengths, we find that there is a periodical oscillation of the BE intensity with respect to polarization angle; and in striking contrast, no periodical variation of CE intensity is observed.

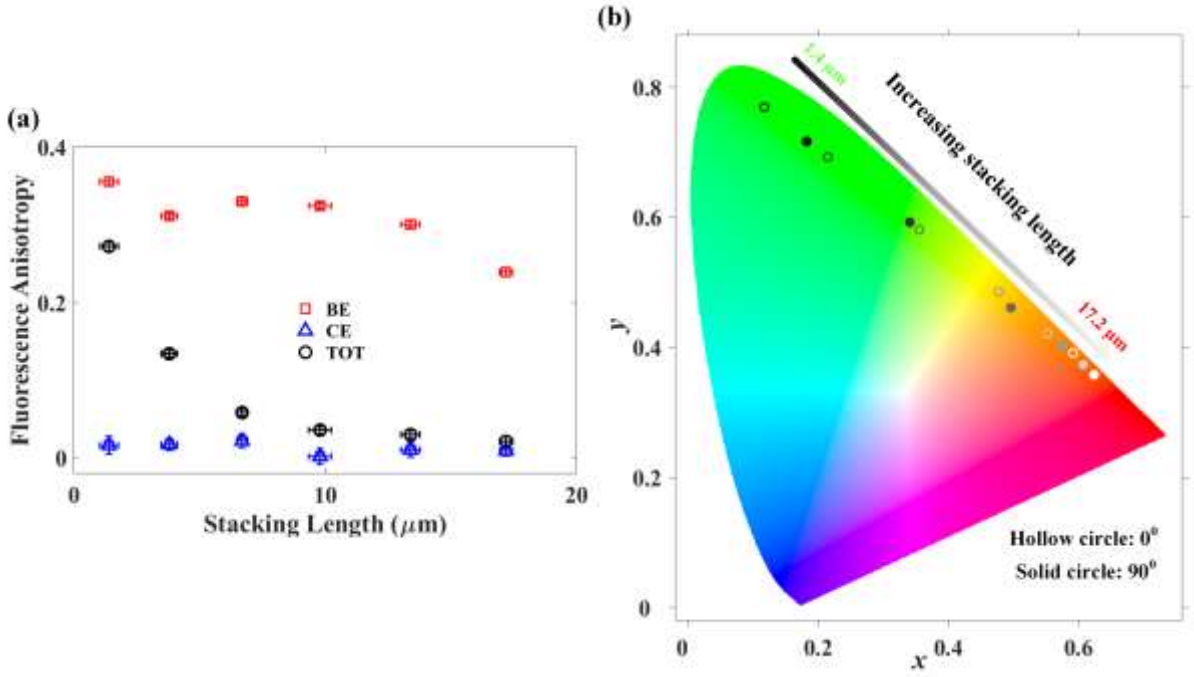

Figure 3. A summary of the achieved controllability. (a) Anisotropy as a function of stacking length for BE, CE and full emission spectra. **(b)** The corresponding colour gamut of the emission colours from the superlattice with different stacking lengths when the polarizer is perpendicular to the principal axis of the superlattice (0˚, the hollow circles) and the polarizer is parallel to the principal axis of the superlattice (90˚, the solid circles).

This discrepancy stems from the different preferences of the transition dipole orientation in BE and CE. It has been widely reported that the electron/heavy-hole exciton transition dipoles in CdSe CQWs are near-perfectly oriented in the platelet plane[12,13]. This pure in-plane dipole orientation can be understood by using the band-edge periodic function ($|u\rangle$). With spin-orbit interaction (here we define the quantum confinement along Z-direction), conduction band electrons have *s*-like symmetry and $|u_e\rangle$ can be written as $|1/2, \pm1/2\rangle$, while heavy-holes hold *p*-like symmetry and $|u_{heavy\text{-}hole}\rangle$ takes $|3/2, \pm3/2\rangle$. We will find that the transition strength (the integral of $\langle u_e|\mu|u_{heavy\text{-}hole}\rangle$) can only be non-zero for dipoles orientated in the platelet plane (i.e., the X-Y plane)[12]. Consequently, in the edge-up configuration (i.e., all platelet planes of CQWs are perpendicular to the substrate and the principal axis in the superlattice), BE (the radiative recombination of electron/heavy-hole exciton) will be the brightest when the principal axis of superlattices is perpendicular to the collection polarizer ($I\_0˚$, the collection polarization is parallel to the excitation polarization) and be the weakest when the principal axis of superlattices is parallel to the collection polarizer ($I\_90˚$, the collection polarization is perpendicular to the excitation polarization).

While for CE (the radiative recombination between the trapped holes and electrons in the host conduction band), transition dipoles do not have any preference and isotropic emission is expected since after the hole is trapped by the copper sites, the Z-projection of total angular momentum is not fixed at ±3/2 anymore and the in-plane conservation has been broken. Similar interpretations can be found in the light-holes ($|u\rangle$ = $|3/2, \pm1/2\rangle$) and spinoff-holes ($|u\rangle$ = $|1/2, 1/2\rangle$), in which the dipole orientation is projected in all space directions[12]. We can also calculate the anisotropy value (R) of BE and CE using[19,37-39]: (I_0° - I_90°)/ (I_0° + 2×I_90°) to quantize the contrast. As shown in **Fig. 3a**, CE yielded an anisotropy value of nearly zero, indicating no net anisotropy (i.e. isotropy). While for BE, with a short stacking length, the anisotropy value is above 0.3, which is comparable to the results in colloidal nanorods[19,39]; with longer stacking length, the anisotropy value decreases to ~0.2 possibly because CQWs are harder to maintain pure edge-up configurations in such a long chain (over 15 μm). Benefitting from the huge anisotropy value contrast in BE/CE, modification of full-spectrum anisotropy will be concomitantly achieved when the intensity ratio between CE and BE is tuned by the stacking length. In **Fig. 3a**, we can see that in the short-stacked superlattice, the full-spectrum is highly anisotropic since BE is dominating the emission spectra, and by the increase of stacking length, the total emission of the superlattice becomes almost isotropic. Moreover, colour coordinates of the two polarizations of emission spectra for six superlattice lengths are plotted in the CIE 1931 chromaticity diagram (**Fig. 3b**), which shows impressive colour controllability ranging from green to red. It is worth mentioning that if proper filters are adopted, such as polarization filters, one can further enhance the colour purity by utilizing the contrast anisotropy values of BE and CE.

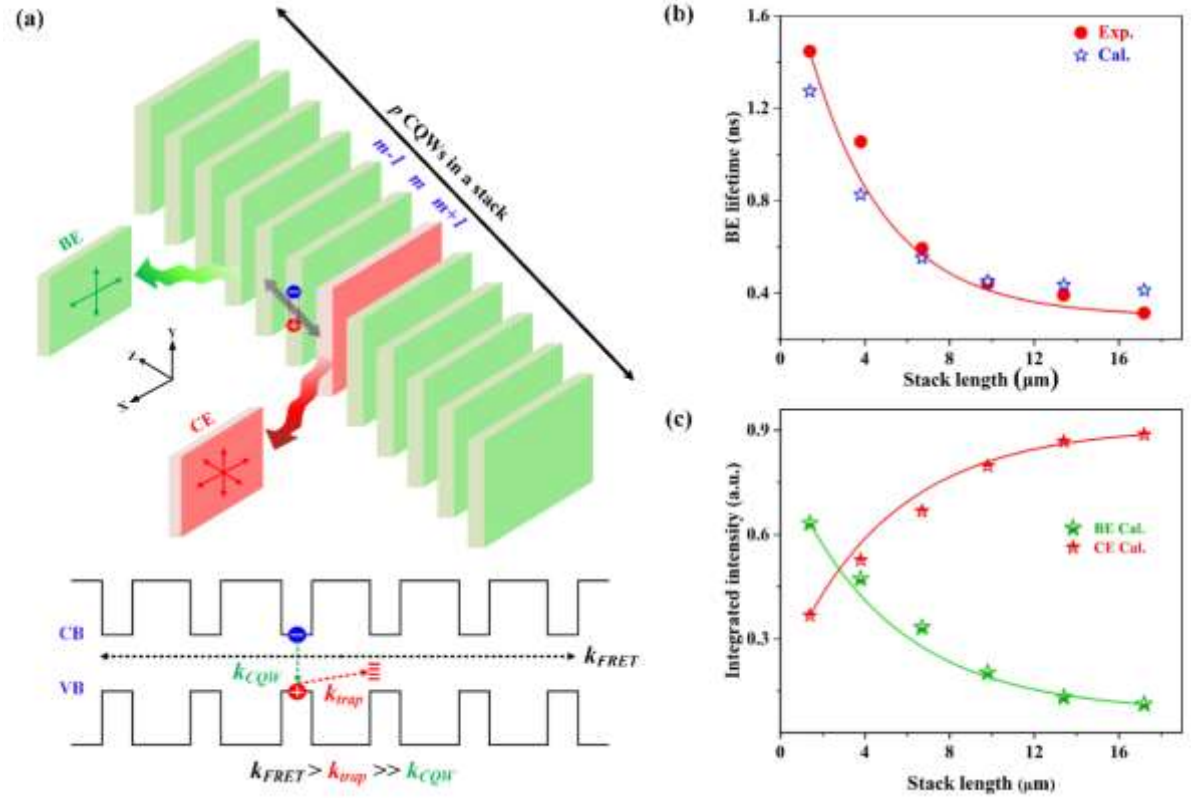

Figure 4. Controlling mechanism in the binary CQW superlattice. (a) Schematic illustration of FRET assisted exciton trapping process in the binary superlattice. Green shaded plates denote undoped CQWs in which BE is greenish and anisotropic due to the in-plane dipole orientation. While red shaded plates represent Cu-doped CQWs in which CE is reddish and isotropic due to the lack of dipole orientation preference. Among all these exciton dynamics, exciton transfer via FRET is the fastest: k_{FRET} is (~ 3 ps)$^{-1}$ and exciton trapping by copper sites has the lifetime of several 10s of picosecond (k_{trap}), the slowest process is band-edge exciton recombination (k_{CQW}), which is in the nanosecond range. **(b)** Correlating the simulated BE lifetime (the hollow stars) with the experimental value (the solid circles) to determine the fraction of the Cu-doped CQW population in the superlattice. The red line is a guide to the eye. **(c)** The calculated BE/CE intensity with various stacking lengths. The agreeable trend exhibits very good support for our mechanism interpretation. The two solid lines are the guides to the eye.

After demonstrating the capability of the stacking length to modify the collective emission colour and anisotropy in superlattices, the remaining task is to clarify the underpinning physics that enable the controllability. Based on our knowledge of CdSe CQWs from previous works, the most reasonable hypothesis is

that the exciton sinking in the Cu-doped CQWs (associated with CE) is boosted by efficient and long-range exciton transfer in superlattices. Let us start with the superlattice constructed by pure undoped CdSe CQWs. Due to the physically close dipole-dipole interaction (various groups have reported a spatial period of < 5 nm in CdSe CQW stacking[11,17,20,22]), pure in-plane dipole orientation and a large self-overlap between the emission/absorption spectra, photoexcited band-edge excitons could transfer back and forth among the adjacent CQWs via Förster resonance energy transfer (FRET), which is a non-radiative exciton transfer process via near-field dipolar coupling. Rowland *et al.* in 2015[15] and Guzelturk *et al.* in 2014[20] reported that the exciton transfer in CdSe CQW stacking can be as fast as ~3 ps with a near-unit efficiency and outpace the Auger recombination. Considering the lifetime of band-edge recombination is around 3 ns, excitons can hop about a thousand times in the column-like assembly before annihilation.

Now we insert the Cu-doped CQWs which behave as the exciton trappers into the stacks, as shown in the schematic illustration in **Fig. 4a**, taking advantage of the multiple transfer loops of band-edge excitons, the copper sites with a hole trapping lifetime of several tens picosecond[23,31] could capture tremendous photo-excited excitons generated in both doped and undoped CQWs. The scenario in our study is an emissive analogue to previous observations that demonstrated emission of chromophores or nanocrystals is quenched in the assembly due to non-emissive trapping assisted by homo-FRET[17,20,40]. As the stacking length is getting longer (i.e., the number of Cu-doped CQWs in the stacking is larger), more of the band-edge excitons will be affected by the exciton trapping process boosted by exciton transfer. As a result, the excitation energy is more likely to be released through the CE channel. We have checked the BE dynamics (probed at 514 nm) of non-stacking CQWs and stacking CQWs with different lengths to support our argument (see **Fig. S3**. The CQWs have a ~2.42-ns average emission lifetime before stacking is induced, which is in accordance with other 4 ML CdSe CQWs reports[13,17,25]. As the superlattice is formed, the average BE lifetime can decrease by an order of magnitude to ~320 ps for the longest stacking. This indicates that the new band-edge exciton consuming channel (i.e., exciton trapping) becomes much stronger with the increase of stacking length.

To further confirm our inference and develop a deeper understanding, we perform a kinetic simulation based on a set of rate equations[17,20,41,42] to reproduce the observed controllability (see the simulation details in **Supplementary Note 1**). For simplicity, we assume the fraction (*f*) of the Cu-doped CQW population within the whole CQW population in all superlattices is fixed (since the superlattice constructed from the uniformly mixed dispersion, the stacking with a considerable amount of CQWs should contain a similar population percentage of doped ingredient) and there is no non-radiative loss in the superlattice. To extract the *f* value in our experiments, we have swept this parameter from 0.01 to 0.20 to correlate the simulated BE dynamics with the measured BE decays in **Fig. S3**, and found acceptable accordance when $f = 0.13$ (as shown in **Fig. 4b**). Then we can determine the photoexcited energy-releasing via BE and CE channels: the BE energy is calculated by integrating the simulated BE dynamics in a relatively long-time window while the CE energy is obtained by subtracting BE photons from the photoexcited photons. The stacking-length-dependent BE/CE intensity from the kinetic model is shown in **Fig. 4c**. Note that we do not expect to achieve good quantitative matching between experiment and simulation results due to the simplification of the model and the random nature of the stacking process. Nevertheless, our simulation results exhibit a good trend in agreement with experimental results: a longer stacking length results in more photoexcited energy released via the CE channel and the collective emission of the superlattice becomes more reddish and isotropic. This again supports our hypothesis that FRET assisted exciton trapping is the dominating mechanism for the collective emission property control.

In summary, we have proposed and demonstrated that the emission properties in a host-guest superlattice consisting of undoped and Cu-doped CQWs is highly controllable through a solvent engineer approach. The physical origin of the controllability lies in the exciton hopping boosted exciton trapping process. As the vertical dimension increases, the ultra-efficient homo-FRET leads to more excitons sinking into the Cu-doped CQWs. Therefore, the copper emission, which is reddish and isotropic, gradually overwhelms the band-edge emission, which is greenish and anisotropic. Moreover, a kinetic model has been developed, which strongly agrees with the observed modulation in our experiments. Given the simplicity and flexibility in tuning collective properties of the superlattice, we anticipate that our work could be, in the future, exploited for practical photonic applications.

Methods

Steady-state optical properties of Cu-doped and undoped dispersion. Absorption spectra of CQWs in hexane are measured by a UV-VIS spectrophotometer (Shimadzu, UV-1800). PL spectra of CQWs in hexane are recorded using a spectrofluorophotometer (Shimadzu, RF-5301PC, excitation wavelength: 355 nm).

Characterization of emission colour and anisotropy in binary CQW superlattice. The excitation source is a 405-nm continuous-wave laser (Cobolt 06-MLD) and the laser spot is focused into the superlattice by a microscope objective (ZEISS, NA = 0.65). The linear excitation polarization is achieved by using the combination of a linear polarizer and a λ/2 wave-plate. The glass substrate hosting superlattices is mounted in a motion stage, which can move along X- and Y-direction to bring different superlattices with various stacking lengths into the field of view, and also can rotate to make sure the principal axis of the superlattice is perpendicular to the excitation polarization. The emission is collected by the same objective in the reflection geometry and the excitation laser was filtered out by a long-pass (LP) filter. Then the emission is passed through the collection polarizer and a 50/50 beam splitter, one path is recorded by a colourful CMOS camera and another path is into the fibre-coupled ANDOR spectrometer (monochromator: ANDOR Shamrock 303i, CCD: ANDOR iDus 401). By rotating the collection polarizer in front of the beam splitter, we can probe the angle-dependent emission colour and anisotropy.

Time-resolved photoluminescence in binary CQW superlattice. The time-resolved PL spectroscopy is performed with a Becker & Hickl DCS 120 confocal scanning FLIM system with the laser pulse at 375 nm with the repetition rate of 20 MHz. For all the time-resolved PL measurements, the collection time is 180 s. Third-order exponential decay models are employed to fit the emission dynamics in Fig. S6 and the instrument response function (IRF) is deconvoluted during the fitting.

Supporting Information

Supporting Figures S1−S3 and Note S1-S2 including the TEM micrograph of 4 ML CdSe undoped CQWs and Cu-doped CQWs; Absorption and PL emission spectra of the binary mixture dispersed in hexane when different amounts of ethanol; Time-resolved BE dynamics of the non-stacking mixture, and the six single superlattices with different lengths; kinetical modelling; synthetic details of undoped and doped CQWs.

Acknowledgements

We would like to acknowledge the financial support from Singapore National Research Foundation under the Program of NRF-NRFI2016-08, the Competitive Research Program NRF-CRP14-2014-03 and the Singapore Ministry of Education AcRF Tier-1 grant (MOE2019-T1-002-087). H.V.D is also grateful to acknowledge additional financial support from the TUBA.

Author Contributions

C.D. and H.V.D. supervised and contributed to all aspects of the research. J.Y. initiated the idea and discussed experiments with M.S. and C.D. in detail. J.Y. wrote the manuscript with the inputs from all authors. With inputs from H.V.D., M.S. designed the doped CQWs and A.S. performed the material synthesis. J.Y. and M.S. performed the experiments to control the degree of stacking. S.D. and H.D.B. conducted the TEM measurement to characterize the stacking. J.Y. and Y.W. conducted the steady-state and dynamic spectroscopy measurements. J.Y. and C.D. performed the kinetic model simulation. All authors analysed the data, discussed the results and commented on the manuscript.

Competing financial interests

The authors declare no competing financial interests.

Data availability

The raw data and processed data are available via reasonable request to the corresponding authors.

References

1. Nie, Z.; Petukhova, A.; Kumacheva, E. Properties and emerging applications of self-assembled structures made from inorganic nanoparticles. *Nat. Nanotechnol.* **2010**, 5, 15–25.
2. Shevchenko, E. V.; Talapin, D. V.; Kotov, N. A.; O'Brien, S.; Murray, C. B. Structural diversity in binary nanoparticle superlattices. *Nature* **2016**, 439, 55–59.
3. Talapin, D. V.; Shevchenko, E. V.; Bodnarchuk, M. I.; Ye, X.; hen, J.; Murray, C. B. Quasicrystalline order in self-assembled binary nanoparticle superlattices. *Nature* **2009**, 461, 964–967.
4. Wang, T.; Zhuang, J.; Lynch, J.; Chen, O.; Wang, Z.; Wang, X.; LaMontagne, D.; Wu, H.; Wang, Z.; Cao, Y. C. Self-assembled colloidal superparticles from nanorods. *Science* **2012**, 338, 358–363.
5. Nagaoka, Y.; Zhu, H.; Eggert, D.; Chen, O. Single-Component Quasicrystalline Nanocrystal Superlattices through Flexible Polygon Tiling Rule. *Science* **2018**, 362, 1396−1400.
6. Nagaoka, Y.; Tan, R.; Li, R.; Zhu, H.; Eggert, D.; Wu, Y. A.; Liu, Y.; Wang, Z.; Chen, O. Superstructures Generated from Truncated Tetrahedral Quantum Dots. *Nature* **2018**, 561, 378−382.
7. Ithurria, S.; Tessier, M. D.; Mahler, B.; Lobo, R. P. S. M.; Dubertret, B.; Efros, A. L. Colloidal Nanoplatelets with Two-Dimensional Electronic Structure. *Nat. Mater.* **2011**, 10, 936−941.
8. Yu, J.; Dang, C. Colloidal Metal Chalcogenide Quantum Wells for Laser Applications. *Cell Rep. Phys. Sci.* **2021**, 2, 100308.

9. Abécassis, B.; Tessier, M. D.; Davidson, P.; Dubertret, B. Self-Assembly of CdSe Nanoplatelets into Giant Micrometer-Scale Needles Emitting Polarized Light. *Nano Lett.* **2014**, 14, 710−715.
10. Tessier, M. D.; Biadala, L.; Bouet, C.; Ithurria, S.; Abécassis, B.; Dubertret, B. Phonon Line Emission Revealed by Self-Assembly of Colloidal Nanoplatelets. *ACS Nano* **2013**, **7**, 3332−3340.
11. Rowland, C. E.; Fedin, I.; Zhang, H.; Gray, S. K.; Govorov, A. .; Talapin, D. V.; Schaller, R. D. Picosecond energy transfer and ultiexciton transfer outpaces Auger recombination in binary CdSe anoplatelet solids. *Nat. Mater.* **2015**, 14, 484−489.
12. Scott, R.; Heckmann, J.; Prudnikau, A. V.; Antanovich, A.; Mikhailov, A.; Owschimikow, N.; Artemyev, M.; Climente, J. I.; Woggon, U.; Grosse, N. B.; Achtstein, A. W. Directed emission of CdSe nanoplatelets originating from strongly anisotropic 2D electronic structure. *Nat. Nanotechnol.* **2017**, 12, 1155-1160.
13. Gao, Y.; Weidman, M. C.; Tisdale, W. A. CdSe Nanoplatelet films with Controlled Orientation of their Transition Dipole Moment. *Nano Lett.* **2017**, 17, 3837−3843.
14. Yu, J.; Hou, S.; Sharma, M.; Tobing, Y. M.; Song, Z.; Delikanli, S.; Hettiarachchi, C.; Zhang, D.; Fan, W.; Birowosuto, M. D.; et al. Strong Plasmon-Wannier Mott Exciton Interaction with High Aspect Ratio Colloidal Quantum Wells. *Matter* **2020**, 2, 1550-1563.
15. Paik, T.; Ko, D.-K.; Gordon, T. R.; Doan-Nguyen, V.; Murray, C. B. Studies of Liquid Crystalline Self-Assembly of GdF_3 Nanoplates by In-Plane, Out-of-Plane SAXS. *ACS Nano* **2011**, 5, 8322−8330.
16. Ye, X.; Chen, J.; Engel, M.; Millan, J. A.; Li, W.; Qi, L.; Xing, G.; Collins, J. E.; Kagan, C. R.; Li, J.; Glotzer, S. C.; Murray, C. B. Competition of shape and interaction patchiness for self-assembling nanoplates. *Nat. Chem.* **2013**, 5, 466−473.
17. Erdem, O.; Olutas, M.; Guzelturk, B.; Kelestemur, Y.; Demir, H. V. Temperature-Dependent Emission Kinetics of Colloidal Semiconductor Nanoplatelets Strongly Modified by Stacking. *J. Phys. Chem. Lett.* **2016**, **7**, 548−554.
18. Momper, R.; Zhang, H.; Chen, S.; Halim, H.; Johannes, E.; Yordanov, S.; Braga, D.; Blülle, B.; Doblas, D.; Kraus, T.; et al. Kinetic Control over Self-Assembly of Semiconductor Nanoplatelets. *Nano Lett.* **2020**, 20, 4102−4110.
19. Cunningham, P. D.; Souza, J. B.; Fedin, I.; She, C. X.; Lee, B.; Talapin, D. V. Assessment of Anisotropic Semiconductor Nanorod and Nanoplatelet Heterostructures with Polarized Emission for Liquid Crystal Display Technology. *ACS Nano* **2016**, 10, 5769-5781.
20. Guzelturk, B.; Erdem, O.; Olutas, M.; Kelestemur, Y.; Demir, H. V. Stacking in Colloidal Nanoplatelets: Tuning Excitonic Properties. *ACS Nano* **2014**, 8, 12524−12533.
21. Boles, M. A.; Engel, M.; Talapin, D. V. Self-assembly of colloidal nanocrystals: from intricate structures to functional materials. *Chem. Rev.* **2016**, 116, 11220–11289.
22. Yu, J.; Sharma, M.; Delikanli, S.; Birowosuto, M. D.; Demir, H. V.; Dang, C. Mutual Energy Transfer in a Binary Colloidal Quantum Well Complex. *J. Phys. Chem. Lett.* **2019**, 10, 5193 − 5199.
23. Nelson, H. D.; Li, X.; Gamelin, D. R. Computational Studies of the Electronic Structures of Copper-Doped CdSe Nanocrystals: Oxidation States, Jahn−Teller Distortions, Vibronic Bandshapes, and Singlet−Triplet Splittings. *J. Phys. Chem. C* **2016**, 120, 5714−5723.
24. Ithurria, S.; Dubertret, B. Quasi 2D colloidal CdSe platelets with thicknesses controlled at the atomic level. *J. Am. Chem. Soc.* **2008**, 130, 16504–16505.
25. Pelton, M.; Ithurria, S.; Schaller, R. D.; Dolzhnikov, D. S.; Talapin, D. V. Carrier cooling in colloidal quantum wells. *Nano Lett.* **2012**, 12, 6158–6163.
26. Biadala, L.; Liu, F.; Tessier, M. D.; Yakovlev, D. R.; Dubertret, B.; Bayer, M. Recombination dynamics of band edge excitons in quasi-two-dimensional CdSe nanoplatelets. *Nano Lett.* **2014**, 14, 1134–1139.
27. Sharma, M.; Gungor, K.; Yeltik, A.; Olutas, M.; Guzelturk, B.; Kelestemur, Y.; Erdem, T.; Delikanli, S.; McBride, J. R.; Demir, H. V. Near-Unity Emitting Copper-Doped Colloidal Semiconductor Quantum Wells for Luminescent Solar Concentrators. *Adv. Mater.* **2017**, 29, 1700821.
28. Sharma, M.; Olutas, M.; Yeltik, A.; Kelestemur, Y.; Sharma, A.; Delikanli, S.; Guzelturk, B.; Gungor, K.; McBride, J. R.; Demir, H. V. Understanding the Journey of Dopant Copper Ions in Atomically Flat Colloidal Nanocrystals of CdSe Nanoplatelets Using Partial Cation Exchange Reactions. *Chem. Mater.* **2018**, 30, 3265-3275 (2018).
29. Yu, J.; Sharma, M.; Li, M.; Delikanli, S.; Sharma, A.; Taimoor, M.; Altintas, Y.; McBride, J. R.; Kusserow, T.; Sum, T. C.; Demir, H. V.; Dang, C.; et al. Low-Threshold Lasing from Copper-Doped CdSe Colloidal Quantum Wells. *Laser Photonics Rev.* **2021**, 2100034.
30. Yu, J.; Sharma, M.; Li, M.; Hernandez-Martinez, P. L.; Delikanli, S.; Sharma, A.; Altintas, Y.; Hettiarachchi, C.; Sum, T. C.; Demir, H. V.; Dang, C. Sustained biexciton emission in colloidal quantum wells assisted by dopant-host interaction. *arXiv* **2019**, 1905.11571.
31. Hughes, K. E.; Hartstein, K. H.; Gamelin, D. R. Photodoping and Transient Spectroscopies of Copper-Doped CdSe/CdS Nanocrystals. *ACS Nano* **2018**, 12, 718−728.
32. Pinchetti, V.; Di, Q.; Lorenzon, M.; Camellini, A.; Fasoli, M.; Zavelani-Rossi, M.; Meinardi, F.; Zhang, J.; Crooker, S. A.; Brovelli, S. Excitonic pathway to photoinduced magnetism in colloidal nanocrystals with nonmagnetic dopants. *Nat. Nanotech.* **2018**, 13, 1145-151.
33. Jana, S.; de Frutos, M.; Davidson, P.; Abécassis, B. Ligand-Induced Twisting of Nanoplatelets and Their Self-Assembly into Chiral Ribbons. *Sci. Adv.* **2017**, 3, No. e1701483.
34. Jana, S. et al. CdSe Nanoplatelets: Living Polymers. *Angew. Chem.* **2016**, 128, 9517 –9520.
35. Jana, S. et al. Stacking and Colloidal Stability of CdSe Nanoplatelets. *Langmuir* **2015**, 31, 10532−10539.
36. Cui, J.; Beyler, A. P.; Coropceanu, I.; Cleary, L.; Avila, T. R.; Chen, Y.; Cordero, J. M.; Heathcote, S. L.; Harris, D. K.; Chen, O.; Cao, J.; Bawendi, M. G. Evolution of the Single-Nanocrystal Photoluminescence Linewidth with Size and Shell: Implications for Exciton-Phonon Coupling and the Optimization of Spectral Linewidths. *Nano Lett.* **2016**, 16, 289−296.
37. Cassette, E.; Mahler, B.; Guigner, J.-M.; Patriarche, G.; Dubertret, B.; Pons, T. Colloidal CdSe/CdS Dot-in-Plate Nanocrystals with 2D-Polarized Emission. *ACS Nano* **2012**, 6, 6741−6750.
38. Sun, M.-J.; Liu, Y.; Wei, Z.; Zhao, Y. S.; Zhong, Y.-W.; Yao, J. Photoluminescent Anisotropy Amplification in Polymorphic Organic Nanocrystals by Light-Harvesting Energy Transfer. *J. Am. Chem. Soc.* **2019**, 141, 6157-6161.
39. Li, Y.; Huang, H.; Xiong, Y.; Richter, A. F.; Kershaw, S. V.; Feldmann, J.; Rogach, A. L. Using Polar Alcohols for the Direct Synthesis of Cesium Lead Halide Perovskite Nanorods with Anisotropic Emission. *ACS Nano* **2019**, 13, 8237−8245.

40. Guzelturk, B.; Olutas, M.; Delikanli, S.; Kelestemur, Y.; Erden, O.; Demir, H. V. Nonradiative Energy Transfer in Colloidal CdSe Nanoplatelet Films. *Nanoscale* **2015**, 7, 2545–2551.
41. Yu, J.; Sharma, M.; Sharma, A.; Delikanli, S.; Demir, H. V.; Dang, C. All-optical control of exciton flow in a colloidal quantum well complex. *Light: Sci. Appl.* **2020**, 9, 27.
42. Yu, J.; Shendre, S.; Koh, W.-k.; Liu, B.; Li, M.; Hou, S.; Hettiarachchi, C.; Delikanli, S.; Hernandez-Martínez, P.; Birowosuto, M. D.; Wang, H.; Sum, T.; Demir, H. V.; Dang, C. Electrically control amplified spontaneous emission in colloidal quantum dots. *Sci. Adv.* **2019**, 5, No. eaav3140.